RESEARCH ARTICLE

Gender Influence on Schizophrenia-Relevant Abnormalities in a Cuprizone Demyelination Model

Brenda Valeiras,[1]* María Victoria Rosato Siri,[1]* Martín Codagnone,[2] Analía Reinés,[2] and Juana María Pasquini[1]

The aim of this study was to determine whether early demyelination can impact behavior in young adulthood. For this purpose, albino Wistar rats of either sex were exposed to cuprizone (CPZ) in two different intoxication protocols: one group was intoxicated before weaning (CPZ-BW), from postnatal day 7 (P7) to P21, through maternal milk, whereas the other group was intoxicated after weaning (CPZ-AW), from P21 to P35. After treatment, rats were returned to a normal diet until P90 when behavioral studies were performed. Both treatments produced marked demyelination in the corpus callosum and retraction of cortical myelin fibers. The subsequent normal diet allowed for effective remyelination at P90. Interestingly, CPZ-AW correlated with significant behavioral and neurochemical changes in a gender-dependent manner. CPZ-AW treatment altered both the number of social activities and the latency to the first social interaction in males, while also highly compromising recognition-related activities. In addition, only P90 males treated AW showed a hyperdopaminergic striatum, confirmed by an increase in tyrosine hydroxylase expression and in dopamine levels. Our results suggest that the timing of demyelination significantly influences the development of altered behavior, particularly in adult males.

GLIA 2014;00:000–000

Key words: cuprizone, myelin impairment, behavioral changes

Introduction

Schizophrenia is a severe psychiatric disorder affecting 0.5–1% of the population worldwide. It is characterized by positive symptoms such as delusional ideas, hallucinations, disordered thinking, often with a later emergence of negative symptoms, including low levels of emotional arousal, mental activity and social drive, and several cognitive impairments, particularly in attention, memory, and executive functions (Kaplan and Sadock, 1971).

Although each theory is supported by evidence, no clear mechanism has so far been able to explain all the alterations in physiological processes associated with schizophrenia. Most studies have originally focused on alterations in neurons and gray matter; however, the fact that more than one brain area is affected, the increased neuronal density and the disconnectivity observed, all suggest that neurodevelopmental problems also occur in white matter, especially in oligodendrocytes (OLGs) and in the myelin that these cells produce. This is strongly supported by the parallelism between age of disease onset and myelination timing.

Several results provide a quantitative cellular correlation of white matter changes in some neuropsychiatric diseases, such us unipolar and bipolar depression or schizophrenia (Hof et al., 2003; Novak et al. 2013; Rajkowska et al., 1999; Torrey et al., 2004; Uranova et al., 2004; Yu et al., 2014). At molecular level, a microarray study comparing the gene expression patterns of schizophrenic and control subjects revealed that the expression of a series of genes related to OLG and myelin were consistently downregulated in schizophrenic brains (Aston et al., 2005; Dracheva et al., 2006; Hakak et al., 2001; Katsel et al., 2005; Tkachev et al., 2003; Shimizu et al., 2014); among others, these genes included myelin-associated

View this article online at wileyonlinelibrary.com. DOI: 10.1002/glia.22704

Published online Month 00, 2014 in Wiley Online Library (wileyonlinelibrary.com). Received Dec 17, 2013, Accepted for publication May 19, 2014.

Address correspondence to J. M. Pasquini, Dpto de Qca Biol, FFyB-UBA-Junín 956, Buenos Aires, Argentina. E-mail: jpasquin@qb.ffyb.uba.ar

From the [1]Department of Biological Chemistry, IQUIFIB, School of Pharmacy and Biochemistry, University of Buenos Aires, CONICET, Buenos Aires, Argentina; [2]Institute of Cell Biology and Neuroscience, Prof. Eduardo De Robertis, CONICET, School of Medicine, University of Buenos Aires, Buenos Aires, Argentina.

*Both these authors contributed equally to this work and should be considered first coauthors.

glycoprotein, myelin basic protein (MBP), proteolipid protein (PLP) (Zhu et al., 2012), and myelin OLG glycoprotein.

The aim of this study was to determine whether early demyelination is able to induce altered behavior in young adult rats. For this purpose, we evaluated two models of cuprizone (CPZ)-induced demyelination differing in the period of intoxication, either from P7 to P21 or from P21 to P35. Our results suggest that both experimental designs can induce cellular and biochemical changes, whereas only the second one correlates with behavioral changes evaluated in adulthood. We have also found differences between sexes that have never been mentioned before in association with the CPZ model. In this scenario, we propose that demyelination develops behavioral alterations characteristic of schizophrenia's symptomatology in young adult male rats.

Materials and Methods

Animals

Albino Wistar rats were housed under 12-h-light/12-h-dark cycles. All efforts were made to reduce the suffering and the number of animals used. Animal care for this experimental protocol was in accordance with the NIH guidelines for the Care and Use of Laboratory Animals. Guides were approved by an *ad hoc* committee of the School of Pharmacy and Biochemistry, University of Buenos Aires.

Experimental Design: CPZ-Induced Demyelination

A group of animals was subjected to a control diet (C). Another group was generated by feeding the mother with pulverized regular chow pellets supplemented with an 0.6% CPZ diet for 2 weeks, (P7–P21); the offspring were named the "CPZ before weaning" (CPZ-BW) group. A third group was fed the same CPZ milled chow for 2 weeks after weaning (P21–P35) (CPZ-AW). All animals were housed with their mothers from birth until weaning at P21. The parameters studied have shown no significant gender differences at P21 and P35; for this reason, the results of two genders were analyzed together. In contrast, significant gender differences were observed in behavioral experiments at P90 when the results were analyzed separately. The experimental design is shown in Fig. 1.

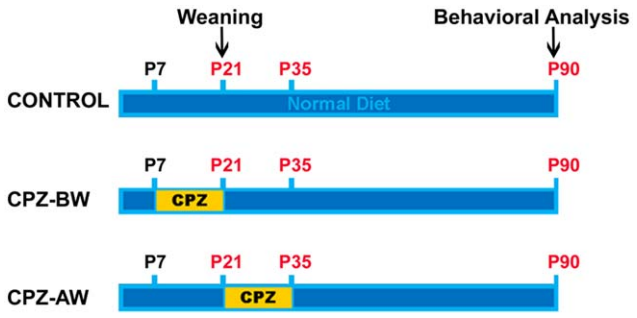

FIGURE 1: Schematic representation of the experimental design. Blue bars represent normal diet, whereas yellow ones show periods when animals were fed a diet containing 0.6% w/w CPZ. For each experimental condition, red labels indicate siblings sacrificed at P21, P35, or P90; brains were then processed for immunohistochemical analyses. For all three groups, behavioral tests were performed at P90. [Color figure can be viewed in the online issue, which is available at wileyonlinelibrary.com.]

Brain Sections

Rats were anesthetized with a xylazine–ketamine mixture (75—10 mg/kg) and intracardiacally perfused with phosphate-buffered saline, pH 7.4, and ice-cold 4% paraformaldehyde. Brains were removed and postfixed overnight at 4°C. Brains were then cryopreserved by placing them in 15 and 30% of sucrose—2 days in each solution—at 4°C before freezing at −80°C or slicing. A cryostat (Leica CM 1850) was used to obtain 30-µm-thick brain coronal sections. The Paxinos and Watson's stereotaxic atlas (Paxinos and Watson, 1986) was used to locate the chosen brain structures eventually. All brain slices were kept at −20°C in a solution containing 50% of glycerol until used for immunofluorescence studies.

Myelin Isolation and Chemical Analysis

Myelin membrane was isolated as described by Norton and Poduslo (1973). The purified myelin was used immediately or stored at −80°C for further analysis. Aliquots of purified myelin were used for the determination of dry weight and total protein (Bradford, 1976) and for protein separation by SDS-PAGE (Laemmli, 1970). Electropherograms were stained with Coomassie Brilliant Blue R-250. Other aliquots were extracted with 2:1 v/v chloroform:methanol according to the methods described by Folch et al. (1957), and the total lipid extract washed was used for the determination of phospholipid (lipid phosphorous) (Chen et al., 1957) and galactolipids (galactose) (Hess and Lewin, 1965). The factors used to calculate the total amount of galactolipids and phospholipids were 4.6 and 24.2, respectively.

Northern Blot Analysis

Total RNA was isolated from myelin fractions of control and CPZ-BW animals at P21. The TRIzol®Reagent method was performed according to the manufacturer's instruction (Life Technologies). RNA concentration was determined by absorbance at 260 nm; purity was evaluated by the A260/A280 ratio; integrity was assessed by ethidium bromide staining (10 mg/mL) under ultraviolet light. RNA (24 mg) was size-fractionated using 1.0% w/v agarose gel containing 18% v/v formaldehyde and later transferred to polyvinylidene difluoride membranes. cDNA probes and blots hybridization were performed as described by Escobar Cabrera et al. (1997).

Immunohistochemistry

Immunohistochemistry was performed as described by Rosato Siri et al. (2013). Primary antibody specifications: anti-MBP (Marker of myelin); Gift from Dr. A. Campagnoni, UCLA; Rabbit, Polyclonal; working dilution (wd) 1:500. Anti-corpus callosum (CC)1/APC (Marker of mature OL); Calbiochem, San Diego, CA; Mouse, Monoclonal; wd 1:100. Anti-GFAP (Marker of astrocytes; Neuromics Antibodies, Edina. CA; Chicken, IgY polyclonal; wd 1:500. Anti-CD11b (Marker of microglial cells); Chemicon International, Temecula. CA; Mouse, IgG monoclonal; wd1:100. Anti-ED1 (Marker of reactive microglia); Neuromics Antibodies, Edina. CA; Mouse, Monoclonal; wd 1:100. Anti-tyrosine hydroxylase (TH) (Marker of dopaminergic neurons); Millipore, Temecula, CA;

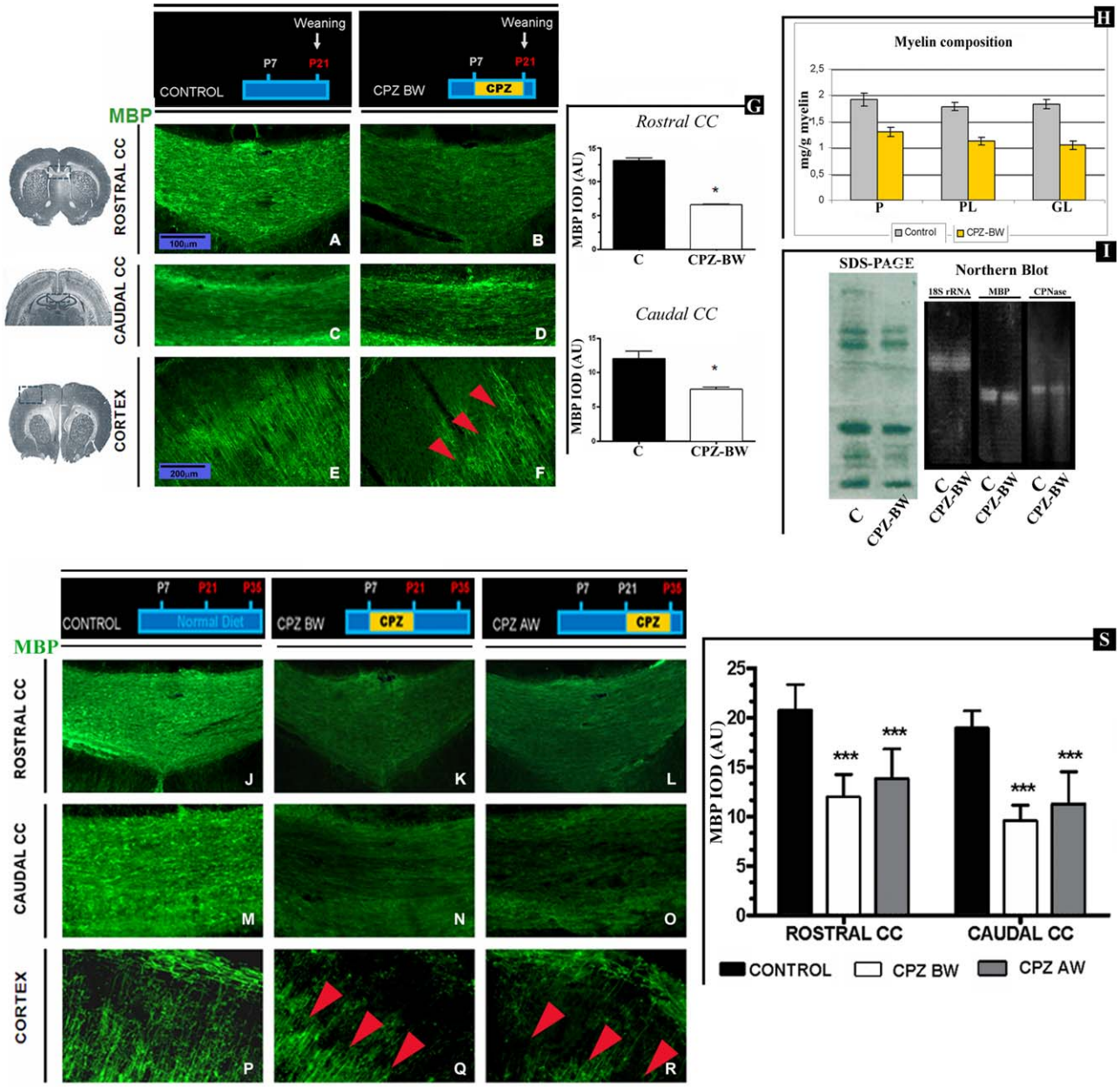

FIGURE 2: MBP immunodetection at P21 and P35. Coronal brain sections of rostral/caudal CC region and frontal cortex from P21 control (A, C, and E), P21 CPZ-BW (B, D, and F), P35 control (J, M, and P), P35 CPZ-BW (K, N, and Q), and P35 CPZ-AW (L, O, and R) animals. G and S: Quantitative data are expressed as the mean IOD ± SD ($n = 12–16$ animals; 4 slices of each animal, 10 randomly selected counting frames of 0.1 mm^2/slice) from rostral and caudal CC regions, respectively. H: Chemical analysis of myelin fractions. I: Myelin protein patterns and expression levels. Loading and transferring were corrected by signal normalized against 18S rRNA. Statistical analyses: one-way ANOVA followed by Tukey's *post hoc* test. Significant differences were observed (compared with control: *$P < 0.05$, *** $P < 0.001$). CC: corpus callosum; cortex: frontal cortex; CPZ-BW: cuprizone before weaning (P7 and P21). P: total myelin proteins. PL: phospholipids of myelin fraction. GL: galactolipids of myelin fraction. CNPase: 2′–3′ cyclic nucleotide 3′-phosphohydrolase. Dotted boxes indicate image location on a representative coronal section. Scale bars: 100 µm (CC) and 200 µm (CORTEX).

Mouse, Monoclonal; wd 1:100. Primary antibody incubation was carried out at 4°C overnight, whereas incubation with the fluorochrome-conjugated secondary antibody was done for 2 h at room temperature. Secondary antibodies anti-rabbit, anti-mouse, or anti-chicken were purchased from Jackson Immunoresearch and were used in a dilution of 1:500; Höechst dye was added together with the secondary antibody solution.

Microscopy and Image Analysis

Digital images were acquired with an Olympus BX50, equipped with a CoolSnap digital camera. Quantitative analysis of MBP and TH immunostaining was performed with the Image ProPlus software by measuring integrated optical density (IOD). CC1+, GFAP+, and ED1+ cells were quantified with Image J by means of the "analyze particle" function; the measurement procedure was applied, allowing

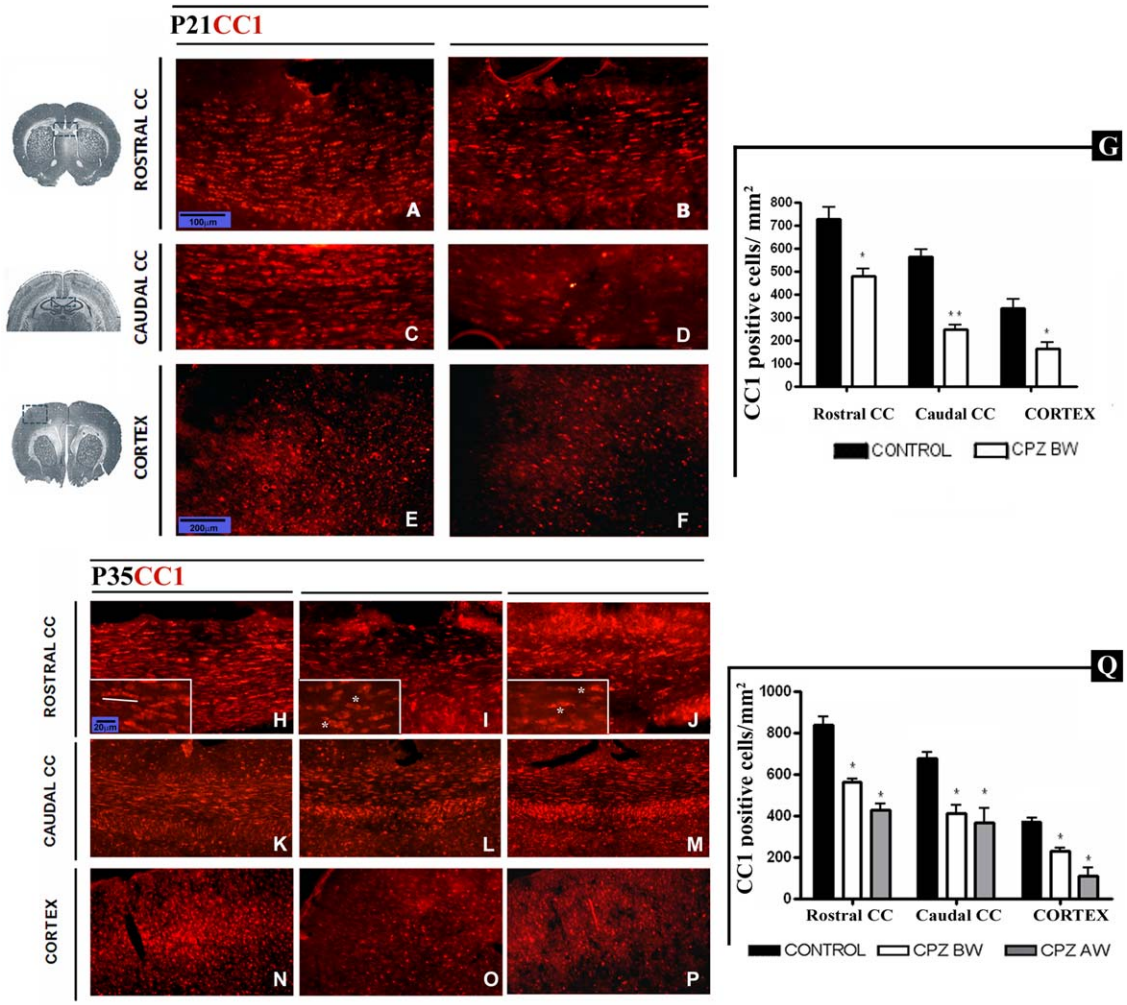

FIGURE 3: CC1 immunodetection at P21 and P35. Coronal brain sections of rostral/caudal CC region and frontal cortex from P21 control (A, C, and E), P21 CPZ-BW (B, D, and F), P35 control (H, K, and N), P35 CPZ-BW (I, L, and O), and P35 CPZ-AW (J, M, and P) animals. G and Q: Quantitative data are expressed as the mean number/field ± SD ($n = 12–16$ animals; 4 slices of each animal, 10 randomly selected counting frames of 0.1 mm²/slice. Statistical analyses: Student's *t*-test with a 95% confidence interval. Significant differences were observed (compared with control: $*P < 0.05$, $**P < 0.01$). Abbreviations, dotted boxes and scale bars are the same as shown in Fig. 2. Boxes: higher magnifications; scale bars, 20 µm. [Color figure can be viewed in the online issue, which is available at wileyonlinelibrary.com.]

for the visualization of on-focus nuclei surrounded by the specific marker. In each experimental group, quantifications were performed by randomly applying counting frames in four slices of each animal.

Concentrations of Dopamine, Serotonin, and Their Metabolites

High-performance liquid chromatography (HPLC)-coupled electrochemical detection (Heikkila et al., 1984) of DA, DOPAC, 5-HT, and 5-hydroxyindolacetic acid was achieved using a Varian 5000 liquid chromatograph coupled to an electrochemical detector (BAS LC-4C). Brains were collected and the striatum dissected, homogenized, and deproteinized in 0.2 N of perchloric acid (1/20). Homogenates were centrifuged and 50 µL of supernatants was injected onto a 12.5-cm × 4 mm Nova-Pak C18 reverse phase column (Waters) developed in 250-mL mobile phase (0.076 M $NaH_2PO_4 \cdot H_2O$; 5.24 mL/L PICB8, 0.99 mM EDTA, and 6% methanol) 1.3 mL/min. Neurotransmitter and their metabolite concentrations were determined on the basis of tissue wet weight.

Behavioral Testing

Locomotor Activity in an Open Field. Locomotor activity was measured using an infrared actimeter (Panlab, Barcelona, Spain). The apparatus consisted of an open field with a plastic enclosure (45 × 45 × 20 cm) surrounded by two square frames, with 16 × 16 infrared emitters each, with an equivalent number of receivers on the opposite walls of the cage connected to a digital counter. The lower and upper frames were placed 2 and 10 cm above the floor, respectively. The test took place in an isolated room between 1:00 and 3:00 p.m. and 24 h before tests, rats were placed in the open field for a 5-min habituation period. Infrared beams were used to detect the movement and the total motor activity of each rat was recorded over a period of 30 min.

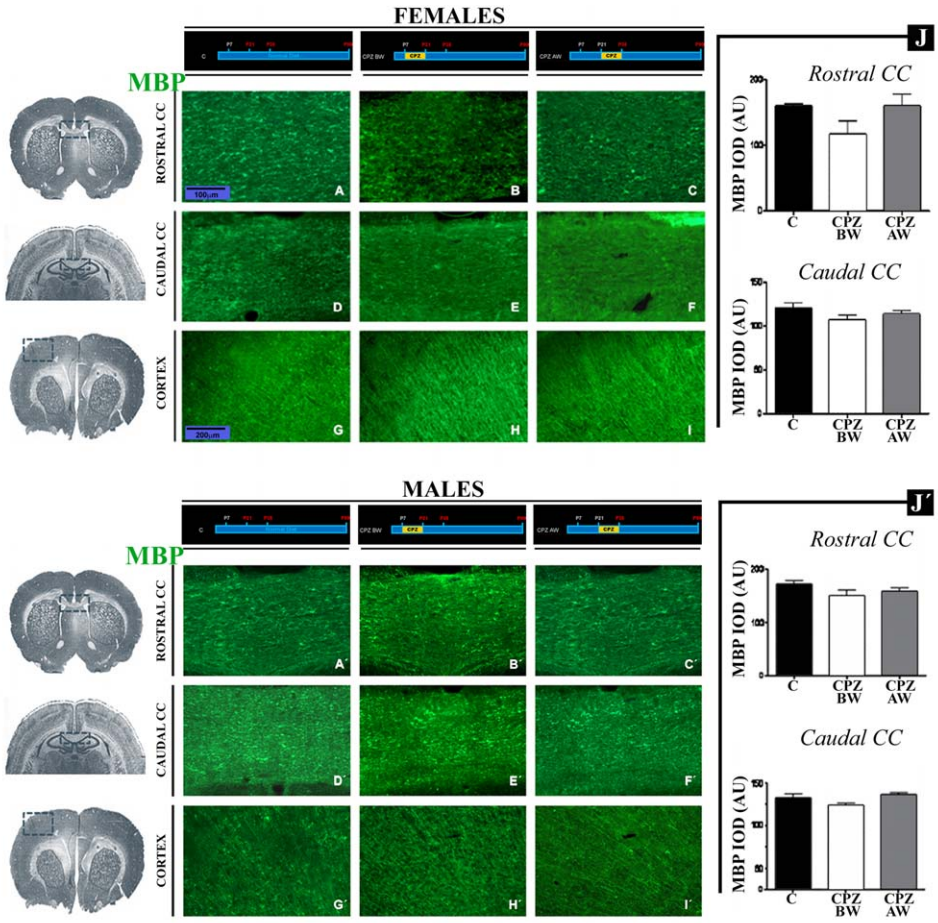

FIGURE 4: MBP immunodetection at P90. Coronal brain sections of rostral/caudal CC region and frontal cortex from control females (A, D, and G) or males (A′, D′, and G′), CPZ-BW females (B, E, and H) or males (B′, E′, and H′), and CPZ-AW females (C, F, and I) or males (C′, F′, and I′). J and J′: Quantitative data are expressed as the mean IOD ± SD ($n = 12–16$ animals; 4 slices of each animal, 10 randomly selected counting frames of 0.1 mm^2/slice from females and males, respectively. Statistical analyses: one-way ANOVA followed by the Newman–Keuls *post hoc* test. No significant differences were observed between groups. Abbreviations, dotted boxes, and scale bars are the same as shown in Fig. 2. [Color figure can be viewed in the online issue, which is available at wileyonlinelibrary.com.]

Exploratory Activity in Open Field. The exploratory activity was assessed in a small open field, previously described by Schneider and Przewłocki (2005). The number of rearings and hole-pokings (animal's nose inside the hole) were measured during a 3-min time session.

Social Behavior. Young adult rats (P90) were tested according to gender in an aquarium measuring 60 × 40 × 40 cm^3 ($l \times w \times h$) with approximately 2-cm-thick wood shaving covering the floor.

The test took place in an isolated room during the dark phase. The aquarium was illuminated by a 40W red light bulb mounted 60 cm above. Four days before the experiment, rats from each group were socially isolated. The stimulus animals were housed in groups of four per cage. The test consisted in placing one isolated animal and one stimulus animal into the test cage for 10 min. Animals were tested in randomized order, and the weight differences between test partners were kept as small as possible. Behavior was assessed for each individual animal. Latency, total duration, and frequency of social exploration and contact were measured, including sniffing or licking any part of the body except the anogenital area, crawling or mounting (standing on hind legs and putting one or two forepaws on the back of the conspecific or climbing over the conspecific), and approaching or following. Anogenital inspection (sniffing or licking the anogenital area of the other rat) was measured separately.

Statistical Analysis. For each experimental group: $n = 12–16$ (four animals from three/four different litters). The corresponding number of animals per treatment, sections per subject, and replicates for consistency are indicated in each figure legend. Data were subjected to parametric tests suitable for normally distributed populations. Statistical analysis was performed using one-way analysis of variance (ANOVA) followed by different *post hoc* tests (GraphPad Prism, GraphPad Software, La Jolla, CA). *P*-values of the different analyses are shown in the figure legends.

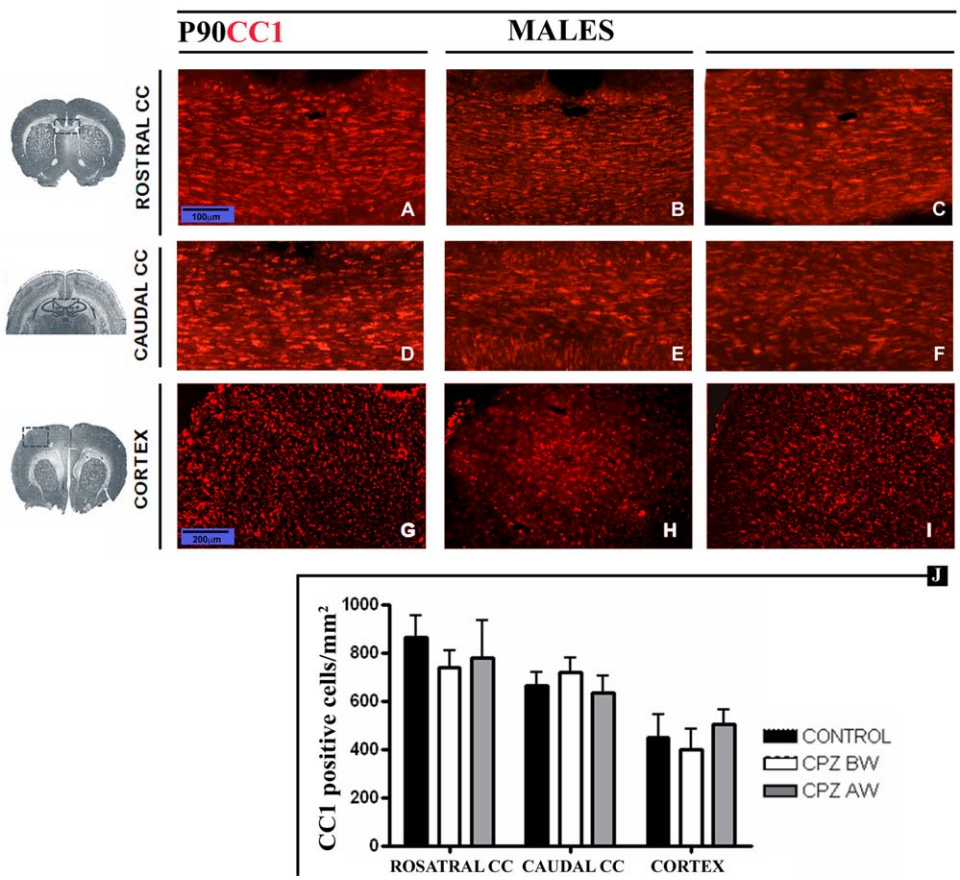

FIGURE 5: CC1 immunodetection at P90. Coronal brain sections of rostral/caudal CC region and frontal cortex from control (A, D, and G), CPZ-BW (B, E, and H), and CPZ-AW (C, F, and I) males. J: Quantitative data are expressed as the mean number/field ± SD ($n = 12–16$ animals; 4 slices of each animal, 10 randomly selected counting frames of 0.1 mm^2/slice. Statistical analyses are the same as shown in Fig. 2. No significant differences were observed between groups. Abbreviations, dotted boxes, and scale bars are also the same as shown in Fig. 2. [Color figure can be viewed in the online issue, which is available at wileyonlinelibrary.com.]

Results

CPZ Intake Produces Demyelination and OLG Loss in Both Experimental Groups

CPZ intake from P7 to P21 (CPZ-BW) resulted in a significant dysmyelination in both the rostral and the caudal region of the CC as shown by reduced MBP immunostaining (Fig. 2B,D,G). Myelin analysis in the frontal cortex (CORTEX), a region known to be affected by CPZ, showed a retraction of myelin tracks at P21 in the CPZ-BW group compared with control animals (Fig. 2E,F; red arrowheads). Additionally, myelin composition and myelin protein patterns were analyzed by SDS-PAGE. The total protein concentration in isolated myelin of CPZ-BW animals decreased by 29.7%; total phospholipids and galactolipids decreased by 35.3 and 42.1%, respectively (Fig. 2H). SDS-PAGE of the myelin fraction revealed a decrease in the relative amount of all myelin proteins (Fig. 2I, left panel). At P21, both MBP and CNPase mRNAs were lower in CZP-BW (Fig. 2I, right panel).

At P35, CPZ-AW animals were significantly demyelinated in both rostral and caudal CC (Fig. 2L,O,S). Interestingly, the loss of myelin in the CPZ-BW group was still pronounced at P35 (Fig. 2K,N,S), 2 weeks after the return to a normal diet. In the CORTEX, myelin tracts were retracted in both CPZ-BW and CPZ-AW respect to control animals (Fig. 2Q,R,P, red arrowheads). At P21, a significant loss in mature OLG, seen as a decrease in the number of CC1+ cells, was observed in the CPZ-BW group as compared with control, both in the rostral and in the caudal regions of the CC (Fig. 3A–D,G). A reduction was also observed in the CORTEX (Fig. 3E,F,G). At P35 this reduction was still observed in the CPZ-BW group (Fig, 3I,L,O,Q). As expected, in CPZ-AW animals at P35, the decrease in the number of CC1+ cells was evident in all the regions analyzed (Fig. 3J,M,P,Q). In all cases, OLG loss was accompanied by an alteration in their characteristic row disposition in the CC (Fig. 3H, box, white line), which generated a more disorganized cell distribution (Fig. 3I,J, boxes, asterisks).

Both CPZ-treated groups exhibited myelin restoration at P90 (Fig. 4). As shown in the quantitative analysis of MBP immunostaining, no significant differences were found between males and females treated with CPZ before or after weaning in

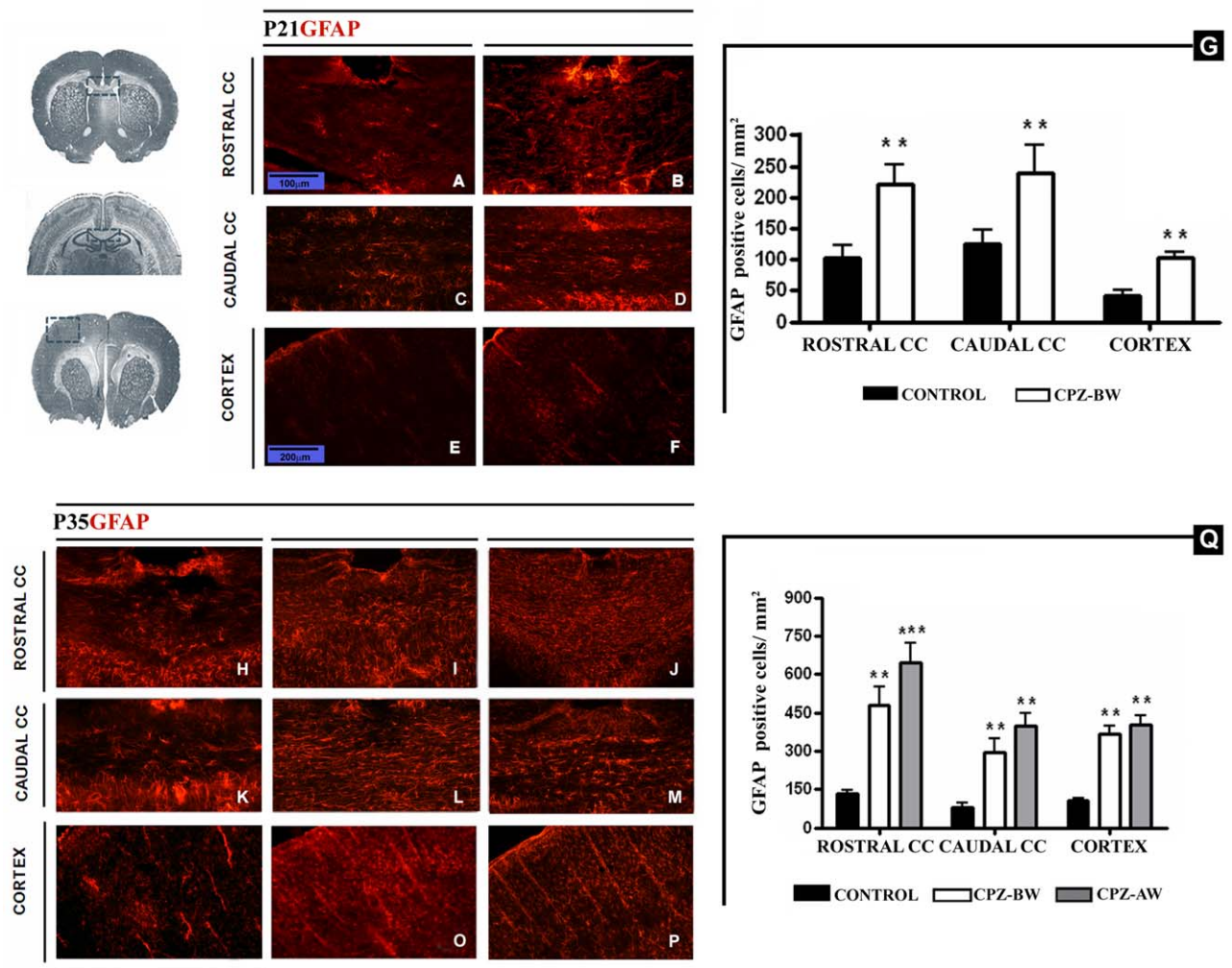

FIGURE 6: GFAP immunodetection at P21 and P35. Coronal brain sections of rostral/caudal CC region and frontal cortex from P21 control (A, C, and E), P21 CPZ-BW (B, D, and F), P35 control (H, K, and N), P35 CPZ-BW (I, L, and O), and P35 CPZ-AW (J, M, and P) animals. G and Q: Quantitative data are expressed as the mean number/field ± SD ($n = 12–16$ animals; 4 slices of each animal, 10 randomly selected counting frames of 0.1 mm^2/slice at P21 and P35, respectively. Statistical analyses are the same as shown in Fig. 2. Significant differences were observed (compared with control: $^{**}P < 0.01$, $^{***}P < 0.001$). Abbreviations, dotted boxes, and scale bars are the same as shown in Fig. 2. [Color figure can be viewed in the online issue, which is available at wileyonlinelibrary.com.]

comparison with control animals, either in the rostral or in the caudal CC. (Fig. 4B,B′,C,C′,E,E′,F,F′,J,J′). Cortical myelin fibers of CPZ-BW and CPZ-AW were restored at P90, reaching the same distances as myelin tracks of control animals in both males and females (Fig. 4H,H′,I,I′). The number of mature OLG was also analyzed with an anti-CC1 antibody. In both males and females of the treated groups at P90, the number of CC1+ cells was comparable to the untreated group. Figure 5 shows representative data from P90 males.

CPZ Treatment Induces Astrogliosis and Microglial Activation

As expected, an increase in GFAP expression was found throughout the CC, rostral, and caudal, as well as in the CORTEX of CPZ-BW compared with control animals at P21 (Fig. 6B,D,F,G). A remarkably high GFAP expression was observed in CPZ-BW at P35, even 2 weeks after the return to a normal diet (Fig. 6I,L,O,Q). This marked astrogliosis was also present in CPZ-AW animals at P35 (Fig. 6J,M,P,Q) as compared with control animals. At P90, the astrocytic population in both treated groups was similar to control animals in males and females (data not shown).

The microglial response was assessed using an anti-CD11b antibody, which detects both quiescent and reactive microglia. At P21, there was an evident change in cell phenotype upon CPZ treatment. Although most CD11b+ cells in the CC of the control group showed the ramified phenotype, characteristic of quiescent, or inactive microglia (Fig. 7A,A′, arrows), the ones in the CPZ-BW group were devoid of branching processes, which is concordant with a reactive microglial phenotype (Fig. 7B,B′, arrowheads). At P35, the abovementioned changes in the phenotype of CD11b+ cells

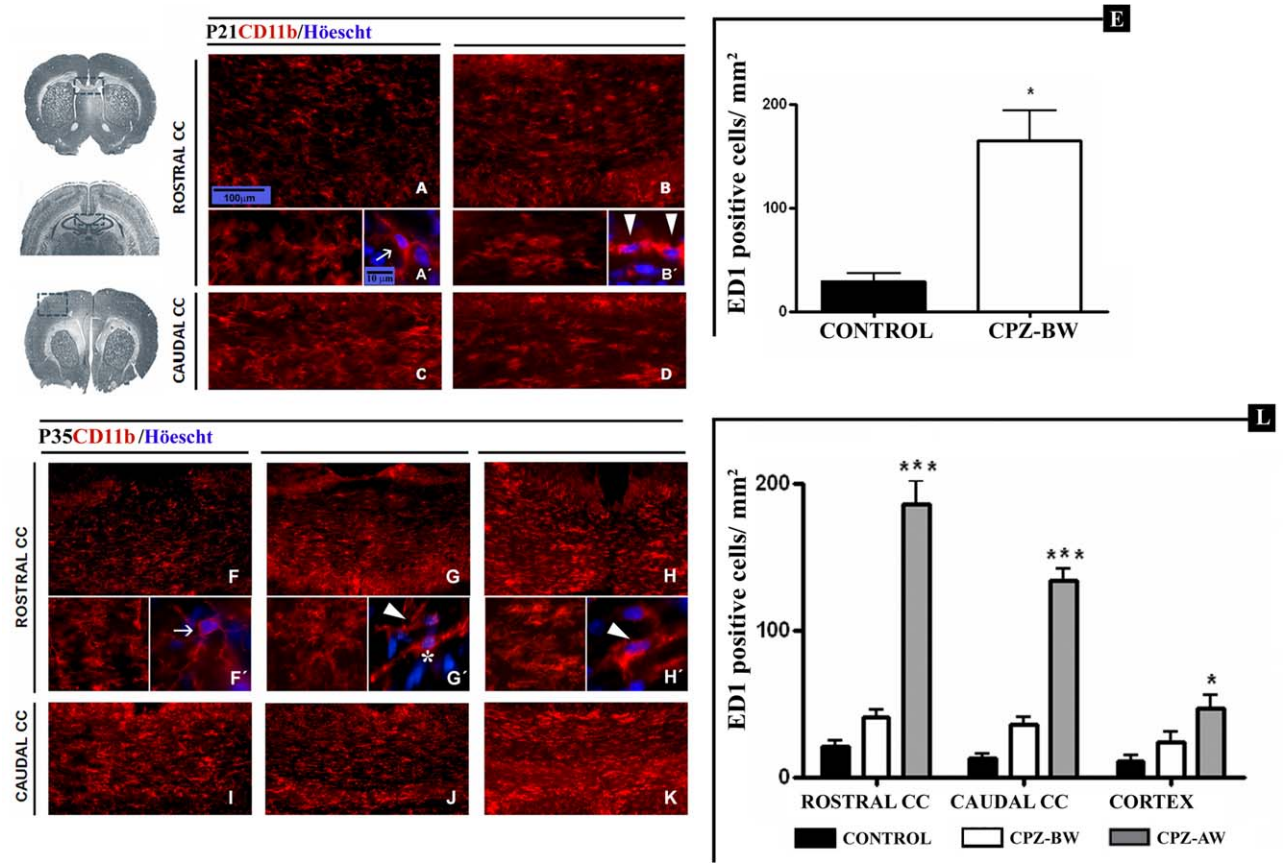

FIGURE 7: CD11b immunodetection at P21 and P35. Coronal brain sections of rostral and caudal CC region from P21 control (A, A′, and C), P21 CPZ-BW (B, B′, and D), P35 control (F, F′, and I), P35 CPZ-BW (G, G′, and J), and P35 CPZ-AW (H, H′, and K) animals (scale bar, 100 μm). Higher magnifications showed morphological differences between quiescent and activated microglial cells (scale bar, 10 μm). E and L: ED1 quantitative data expressed as the mean number/field ± SD ($n = 12–16$ animals; 4 slices of each animal, 10 randomly selected counting frames of 0.1 mm²/slice at P21 and P35, respectively. Statistical analyses: Student's *t*-test with a 95% confidence interval (for P21) and one-way ANOVA followed by Tukey's *post hoc* test (for P35). Significant differences were observed (compared with control: *$P < 0.05$, *** $P < 0.001$). Abbreviations and dotted boxes are the same as shown in Fig. 2. [Color figure can be viewed in the online issue, which is available at wileyonlinelibrary.com.]

were also observed in the CPZ-AW group with predominance of rod-like reactive microglia (Fig. 7H,H′, arrowhead). In contrast, in the CPZ-BW group, the CD11b+ population was composed of both an intermediate phenotype with few branches and the reactive microglial cells (Fig. 7G′, asterisk arrowhead, respectively). The quantitation of these reactive microglial cells was performed, using ED1 as an exclusive marker of this phenotype, at P21 and P35 (Fig. 7E,L, respectively). In both P90 males and females, CD11b+ cells were found to be similar in morphology and number, for all the three experimental groups. In all cases, the predominant cell phenotype corresponded to ramified inactive microglia, confirmed by higher magnifications (Fig. 8, arrows).

CPZ, TH-Immunoreactive Fibers, and Dopamine in the Globus Pallidus

For further analysis, the expression of TH, a widely used marker of dopaminergic neurons, was evaluated in the striatum owing to its key involvement in dopaminergic pathways. The analysis was particularly focused on the globus pallidus (GP), which involves less condensed TH+ fibers than the caudate putamen and hence facilitates the identification of possible differences by immunohistochemistry. Among P90 males, both CPZ-treated groups exhibited higher density of TH-immunoreactive fibers in the GP, the CPZ-AW group showing a greater difference from control animals (Fig. 9B′,C′,D′). In contrast, TH expression in both CPZ-treated groups of P90 females was similar to that of the control group (Fig. 9B,C,D).

On the basis of these results, dopamine concentrations were evaluated only in P90 control and treated males. To this end, the whole striata were dissected and the concentrations of dopamine and its metabolite were determined by HPLC. The concentrations of dopamine were increased in both CPZ-BW and CPZ-AW males as compared with controls (Fig. 9E). However, the most pronounced and statistically significant difference was found in the CPZ-AW group. The same tendency was

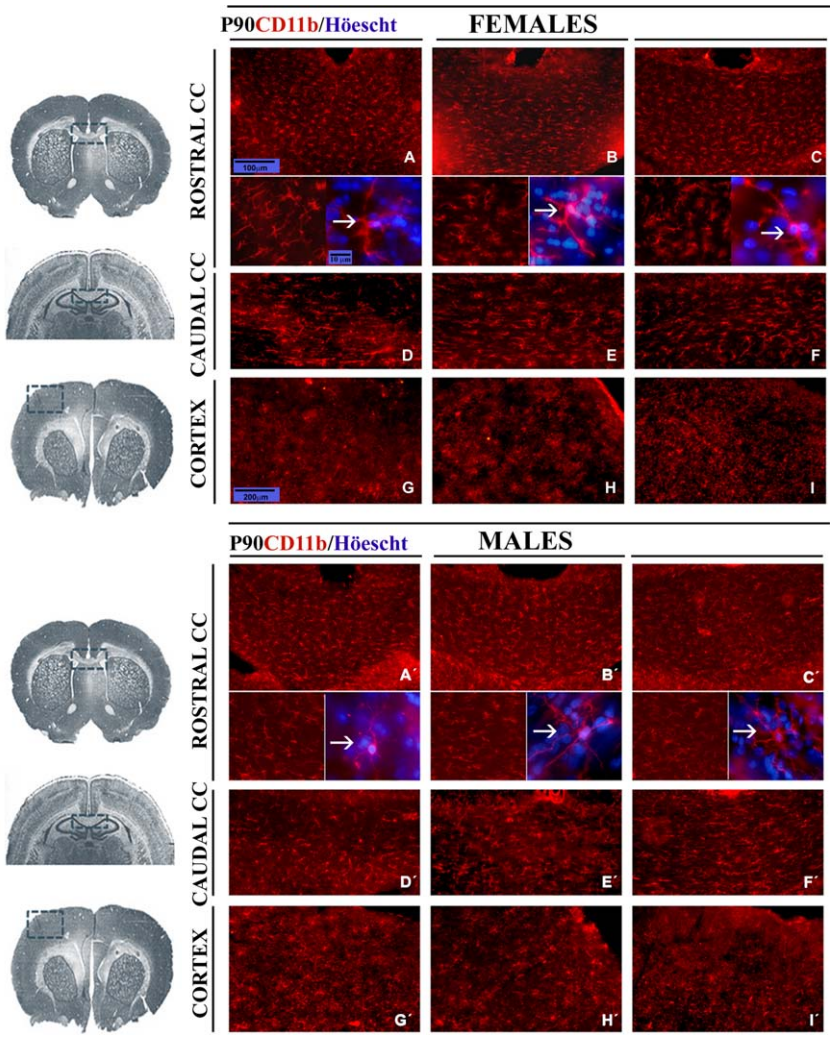

FIGURE 8: CD11b immunodetection at P90. Coronal brain sections of rostral/caudal CC region and frontal cortex from control females (A, D, and G) or males (A′, D′, and G′), CPZ-BW females (B, E, and H) or males (B′, E′, and H′), and CPZ-AW females (C, F, and I) or males (C′, F′, and I′). Abbreviations, dotted boxes, and scale bars are the same as shown in Fig. 2. Higher magnifications are also the same as shown in Fig. 7. [Color figure can be viewed in the online issue, which is available at wileyonlinelibrary.com.]

observed in dopamine's metabolite, DOPAC (Fig. 9E′). The concentration of serotonin was also studied and although there was a mild increase in serotonin levels in CPZ-AW animals, this difference was not statistically significant. As regards serotonin's metabolite, 5HIIAA, concentrations in both treated groups were comparable to those of untreated males (data not shown).

Behavioral Analysis

CPZ Treatments Differently Affect Locomotion in Male and Female Rats at P90. The total locomotor activity of males from the treated groups was not statistically different from the control group in any of the six intervals analyzed (Fig. 10A′). When activity in the central compartment of the open field was analyzed, an increase in males from the CPZ-AW group was found although this was seen only during the first interval (Fig. 10B′). In contrast, both CPZ treatments increased locomotor activity in female rats, particularly owing to increased activity in the central compartment during intervals 1 and 2 (Fig. 10A,B).

Exploratory activity was evaluated as the number of total exploratory events, number of rearings or hole-pokings, and the contribution of each of these exploratory events to the total activity. Results showed that the exploratory activity was not affected in a significant way by any CPZ treatment either in males or in females (data not shown).

Different Social Behavioral Alterations in CPZ-Treated Males and Females. In analyzing social behavior, a tendency to a decrease was found in the number of social events and an increment was observed in the latency to the first social interaction in CPZ-AW males (Fig. 11A′,B′). These

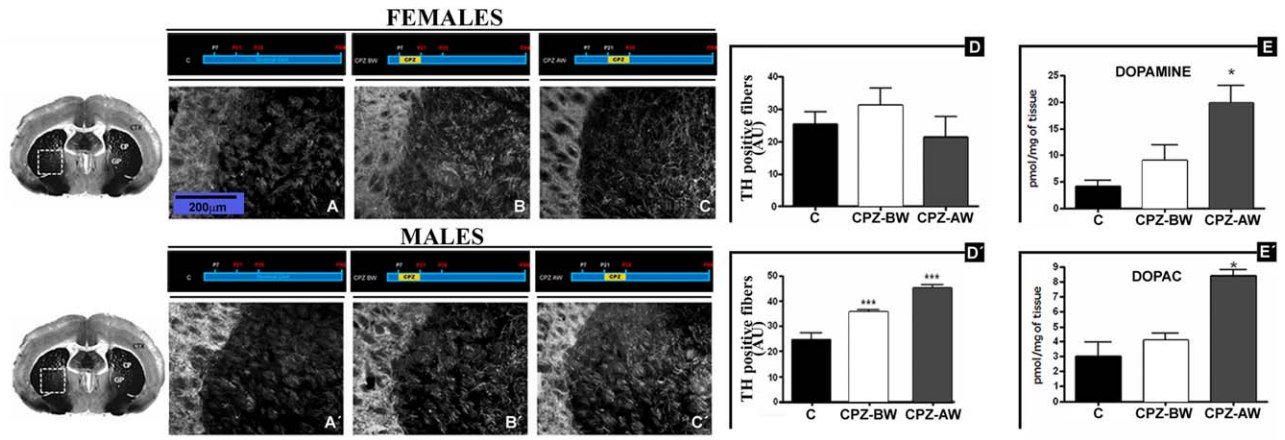

FIGURE 9: Immunohistochemical analysis of TH-positive fibers and dopamine levels in the GP at P90. Coronal brain sections of striatum from control (A and A′), CPZ-BW (B and B′), and CPZ-AW (C and C′) females and males, respectively (scale bar, 200 μm). D and D′: Quantitative data are expressed as the mean IOD ± SD ($n = 12–16$ animals; 4 slices of each animal, 10 randomly selected counting frames of 0.1 mm^2/slice. Statistical analyses are the same as shown in Fig. 2. Significant differences were observed compared with control group: *$P < 0.05$, ***$P < 0.001$. E and E′: Concentration of striatal dopamine and its metabolite, respectively. Data are expressed as pmol/mg ($n = 4$ animals for each group). [Color figure can be viewed in the online issue, which is available at wileyonlinelibrary.com.]

tendencies were not seen in female rats after any of the CPZ treatments (Fig. 11A,B).

The analysis of recognition-related social activities revealed that the number of anogenital inspections in male rats was equally decreased by the CPZ-BW and CPZ-AW treatments (Fig. 11C′). Interestingly, only CPZ-AW males showed a reduction in the total time spent in this activity (Fig. 11E′), together with a decrease in the mean duration of each social recognition event (Fig. 11D′). In contrast, anogenital inspection frequency was not affected by any treatment in female rats (Fig. 11C) although a decrease in the mean duration of each event and in the total time spent in sniffing/licking activities was registered in CPZ-AW female rats (Fig. 11D,E). When analyzing other social activities such us following/approaching, mounting, crawling, and play behavior, changes were observed in CPZ-AW but not in CPZ-BW rats. In addition, the CPZ-AW treatment induced a marked reduction in the total number of crawlings in males (Fig. 12A′). In accordance, the total time spent in this activity was markedly reduced although the duration of each crawling event remained unchanged (Fig. 12C′,12B′). In contrast, the CPZ-AW treatment increased the total duration of following–approaching events in females (Fig. 12C).

Discussion

There has been a relatively recent shift in the field of schizophrenia research, moving from the traditional perspective of gray matter and altered neurocircuitries, to a new point of view involving white matter and OLG damage (Chew et al., 2013). This is strongly supported by new brain imaging studies which have revealed not only gray matter atrophia, but also white matter deficits in the frontal and temporal lobes (Janssen et al., 2008; Lui et al., 2009; Schneiderman et al., 2009). Furthermore, postmortem histological examinations have shown demyelination or OLG apoptosis in schizophrenic patients (Aberg et al., 2006; Flynn et al., 2003; Stewart and Davis, 2004; Uranova et al., 2011). In addition, increasing results have shown that schizophrenia is a neurodevelopmental disorder attributed to genetic and environmental factors (Meyer et al., 2008; Murray et al., 1992; Weinberger, 1995) that affect normal brain development and significantly contribute to an increase in the risk of schizophrenia in adulthood (Duce et al., 2008; Smith, 1992; Wright and Murray, 1993).

This study is mainly focused on investigating whether the timing of demyelination influences the appearance of abnormal behavior in adult animals. For this purpose, we evaluated the effects of two different CPZ-induced demyelination protocols (CPZ-BW and CPZ-AW) and their similarity to schizophrenia symptoms. The effective demyelination observed in the CPZ-AW group has been previously described by our laboratory. In preliminary studies, our group has analyzed the effects of CPZ fed to P21 rats at different doses and during 1, 2, and 3 weeks. We found that CPZ administered in the diet during 2 weeks at a dose of 0.6% was effective in producing clear biochemical and histological evidence of demyelination in young rats (Adamo et al., 2006). Franco et al. (2008) have published that, in CPZ-fed rats at P35, the CC showed clear signs of demyelination when compared with normal controls. At P37, in spite of the fact that CPZ had been removed from the diet, severe demyelination was still present. At variance with mice, maximum demyelination in rats was histologically detected at P42 (1 week after treatment). Histological signs of remyelination were first observed at P49 (2 weeks after treatment) and progressive recovery was observed till P56. In contrast, the fact

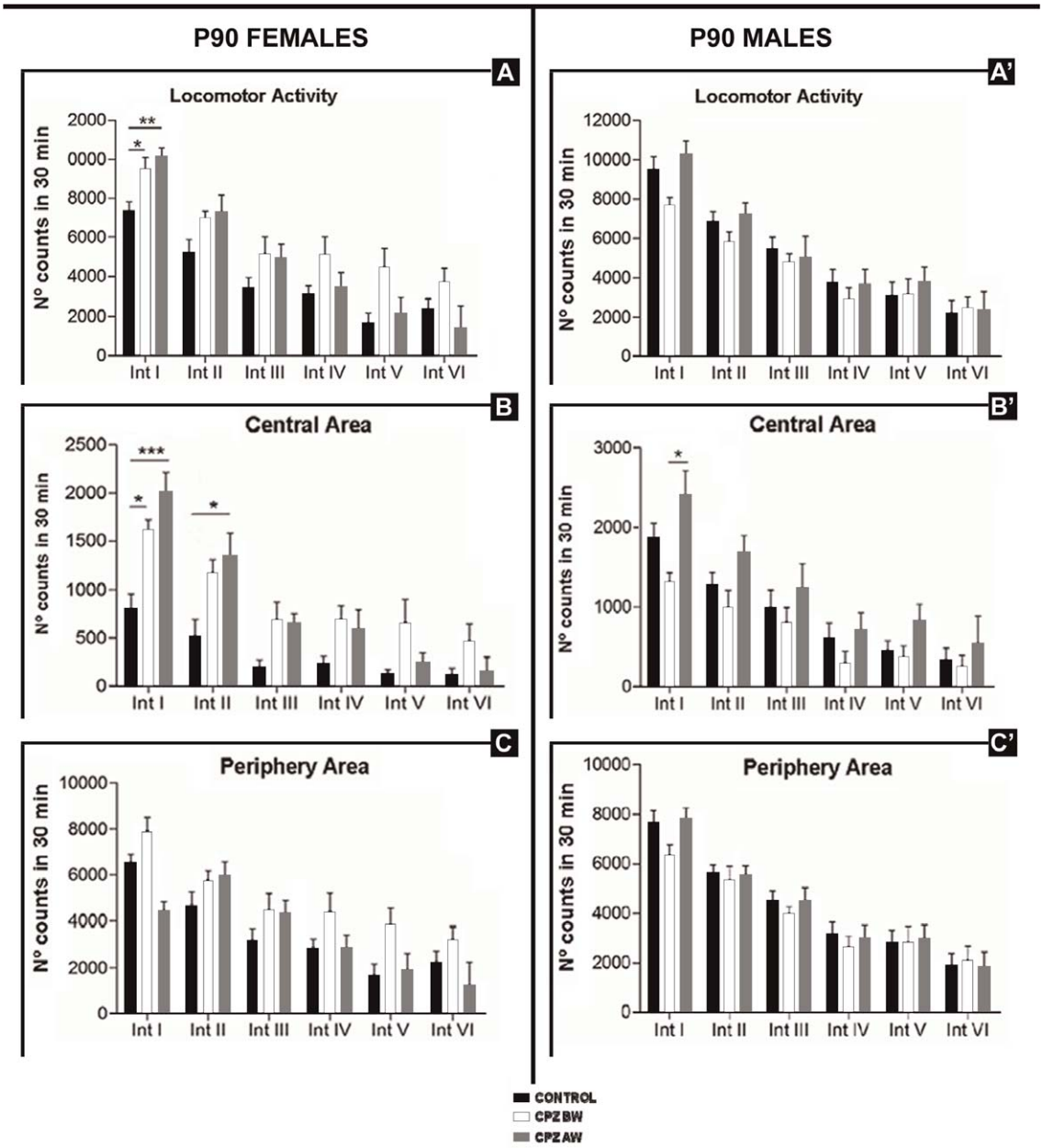

FIGURE 10: Locomotor activity in females and males. Total locomotor activity in the whole area (A and A′), in the central area (B and B′), and in the periphery (C and C′) for females and males, respectively ($n = 12–16$). Statistical analyses: one-way ANOVA followed by the Tukey–Kramer *post hoc* test. Significant differences were observed compared with control group: *$P < 0.05$, **$P < 0.01$, and ***$P < 0.001$.

that CPZ treatment in the earliest postnatal period (P7–P21) affects myelin formation is itself a novel finding. In addition to abnormal myelin deposition, we observed anomalous myelin composition, both similar to those found in rats after weaning, as well as comparable myelin loss in both experimental conditions. The myelin impair observed in CPZ-BW pups might indicate that a metabolite of CPZ (still not known) reaches the milk and induces OLG damage.

Along with the well-described increase in the population of OLG precursors (Adamo et al., 2006; Rosato Siri et al., 2013), CPZ generates a deleterious effect on mature OLG (Bénardais et al., 2013; Matsushima and Morell, 2001). CPZ administration before weaning coincides with the ontogenetic myelination process and may dramatically affect the few mature OLG present at this moment and the ones concomitantly maturing, thus producing dysmyelination or a delay in ontogenetic myelination rather than demyelination. Interestingly, the astrogliosis induced by CPZ was maintained long after (2 weeks) CPZ removal, together with the characteristic change in microglial morphology and their activation (seen by CD11b and ED1markers). It is worth mentioning that recent study (Blank and Prinz, 2013) has shown that, in

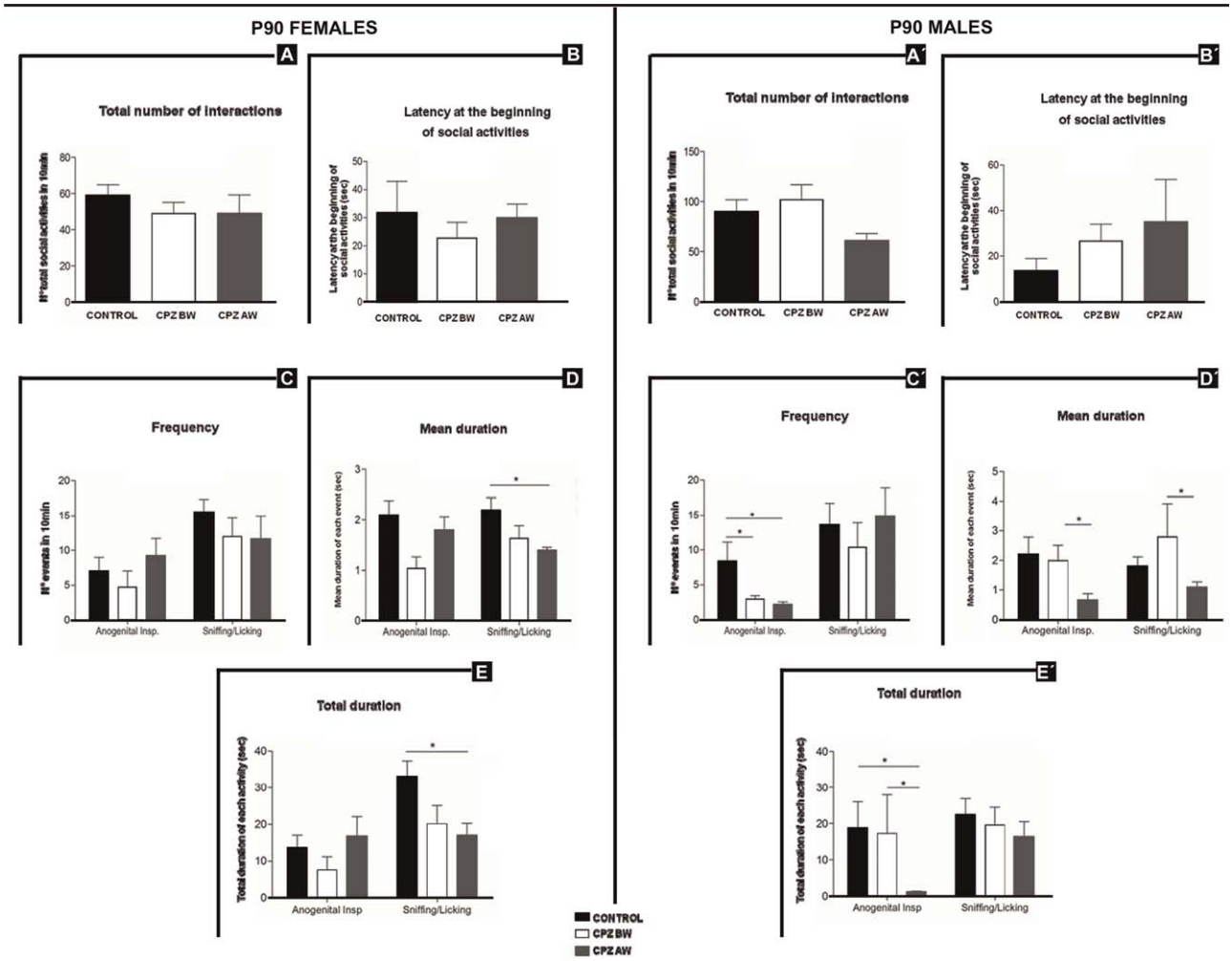

FIGURE 11: Social behavior in females and males. Number of total interactions (A and A′) and latency at the beginning of social activities (B and B′) for females and males, respectively ($n = 12–16$). Statistical analyses: one-way ANOVA followed by Tukey–Kramer *post hoc* test. No statistical significance was found. Sniffing/licking and anogenital inspection frequency (C and C′), mean duration of each event (D and D′), and total duration (E and E′) for females and males, respectively ($n = 12–16$). Statistical analyses: one-way ANOVA followed by Tukey–Kramer *post hoc* test. Significant differences were observed compared with control group: *$P < 0.05$.

neuropsychiatric disorders, microglia do not only have immunomodulatory functions but also play an active role in synaptic formation. Our data could then indicate that, in a CPZ-BW scenario, the subsequent myelination process, although slower, resembles the developmental process in a more proficient way while not compromising the physiological formation of neural circuits. In contrast, 2-week CPZ withdrawal in the CPZ-AW treatment leads to an explicit myelin structural recovery (Matsushima and Morell, 2001; Stidworthy et al., 2003) with some particular biochemical alterations. For instance, TH showed differences between genders, with a significantly higher level in CPZ-AW males. Also, the measurement of dopamine concentrations in the striatum of P90 males rendered the highest levels in the CPZ-AW group, whereas treated females had TH and dopamine concentration levels similar to control animals. Finally, high dopamine levels have been related to hyperlocomotion although we were unable to find this behavioral feature in males.

The newest tendency in schizophrenia research is to link OLG and myelin dysfunction with neurocircuitry abnormalities. Some models have already been proposed on how demyelination might induce the hyperdopaminergic state found in schizophrenic patients, involving a misbalance in glutamate as well (Rosin et al., 2005; Takahashi et al., 2011). In accordance, this study can establish a link between a demyelination model, including retraction of cortical myelin fibers, and the enduring "dopamine theory of schizophrenia," through the finding of high dopamine levels in the striatum of CPZ-treated males. As the two different CPZ-induced demyelination treatments clearly exposed a time-dependent effect, and to validate the neurodevelopmental theory, it is crucial to determine a time-responsive period. In accordance with other studies

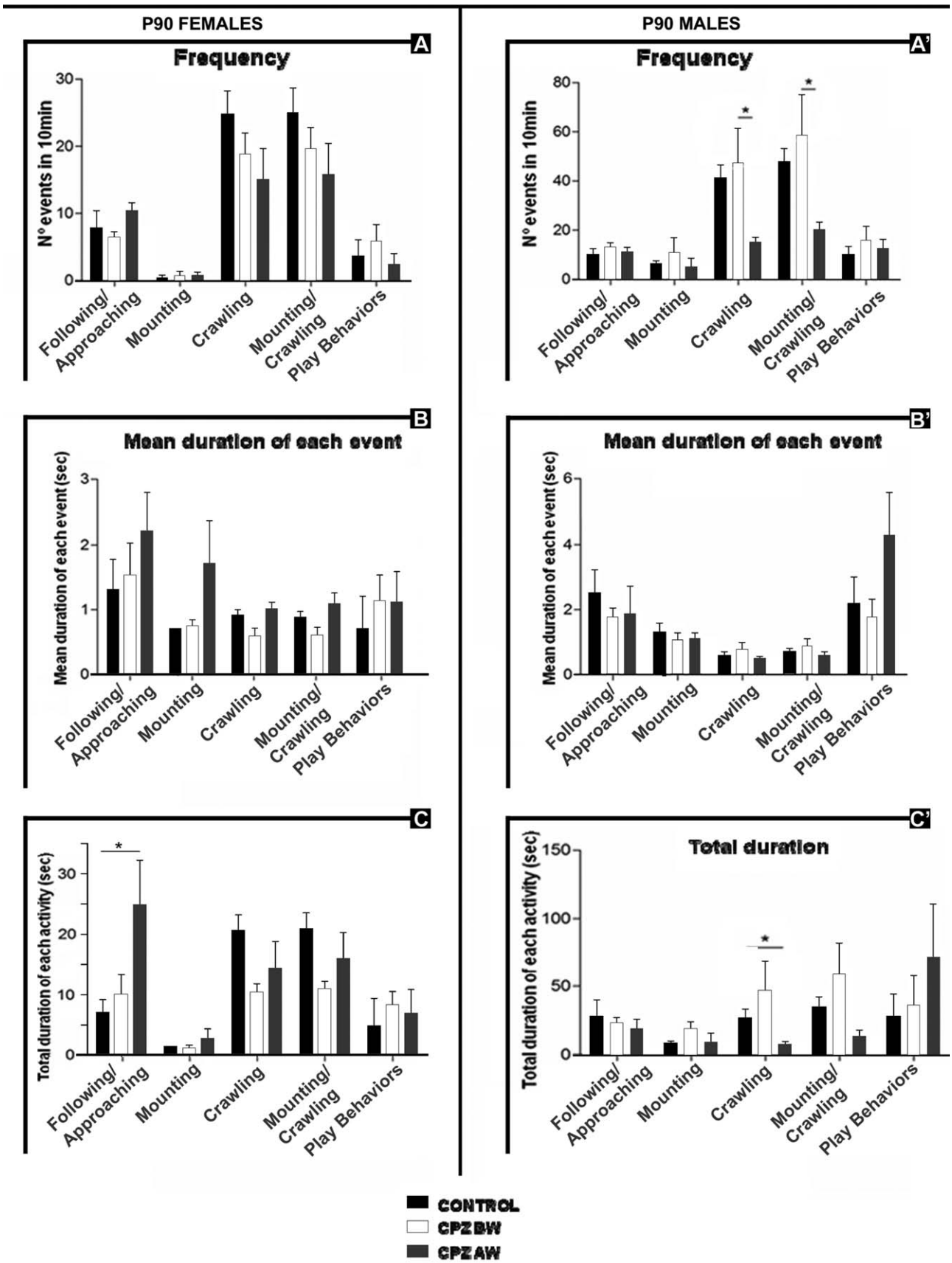

FIGURE 12: Social behavior in females and males. Following/approaching, mounting, crawling, and play behavior. Frequency (**A** and **A′**), mean duration of each event (**B** and **B′**), and total duration (**C** and **C′**) for females and males, respectively ($n = 12–16$). Statistical analyses: one-way ANOVA followed by Tukey–Kramer *post hoc* test. Significant differences were observed compared with control group: *$P < 0.05$. In accordance with the low mounting frequency found in females, values from control group in (B and C) have no standard deviation because they correspond to the events from the only animal that showed this behavior.

(Makinodan et al., 2009, 2012), our results strongly suggest that the period between P21 and P35 involves a more complete and less plastic cytoarchitecture, which makes it a critical time window.

To search for a possible correlation between our demyelination models and schizophrenia, behavioral tests were performed at P90. In accordance with schizophrenia symptomatology, CPZ-AW treatment was the most powerful in affecting several aspects of social behavior in males but not in females. Different from CPZ-BW, the CPZ-AW treatment altered both the number of social activities and the latency to the first social interaction in males, while also highly compromising recognition-related activities and crawling events. Indeed, CPZ-AW females showed a paradoxical increase in the time spent in following/approaching activities. These profound differences between male and female behavioral performances seem highly relevant as schizophrenia appears to have higher incidence among males (Aleman et al., 2003; McGrath et al., 2004, 2008) although the reason for this differential susceptibility remains unclear. On the basis of gender differences recently found in the cognitive functions of patients with chronic schizophrenia (Han et al., 2012), it is believed that the explanation might reside in subtle changes in neurotransmission, connectivity, and neural electric activity (Patel et al., 2013). In addition, our study is the first to show that the timing of demyelination (CPZ-BW vs. CPZ-AW) differently affects behavior in a gender-dependent manner.

Regarding the anxiety frequently observed in schizophrenic patients (Achim et al., 2013; Braga et al., 2013; Dernovsek and Sprah, 2009), it should be mentioned that CPZ-AW animals exhibited a reduced anxiety index (reduced thigmotaxis) in the open field test. However, this reduction could hardly be taken as an anxiolytic trait as it was restricted to the initial interval characterized by novelty-induced exploration (Simon et al., 1994).

As regards differences between our two experimental groups, another question remains as to why the effect on behavior is more pronounced in CPZ-AW than in CPZ-BW animals and, at this point, it should be remembered that both models produced very similar changes in myelin composition. A study by Makinodan et al. (2009) showed that CPZ treatment between P29 and P56 in mice leads to long lasting abnormal behavior in spite of remyelination, which may be owing to the plasticity of developing neural circuits. As previously known, myelin has a major role in the formation of neural circuits and, in this context, authors speculate that myelination between P29 and P56 could be critical for the formation of neural circuits in brain areas such as the PFC, which is in fact myelinated later than other brain regions. This could also explain the effect of CPZ-AW in our study, considering the comparable intoxication period (P21–P35) used by Makinodan et al. (2009). The demyelination disclosed in CPZ-AW animals at P35 might be the initial cause of abnormal behavior at P90, primarily because of secondary and more permanent defects in neural circuits. This was also supported by the alterations observed in the dopamine pathway in adult CPZ-AW males, with striatal hyperdopaminergia persistent at P90. The reason why the neurocircuitries of rats treated before weaning could be less affected by CPZ is another point of interest. On the basis of the more pronounced dysmyelination or retarded myelination observed in immunohistochemical characterization, CPZ-BW animals might have been expected to present more abnormal behavior (Novak et al., 2013); however, although their behavior was indeed affected, the effect was less marked than in the case of CPZ-AW animals.

Even if CPZ cannot fully reflect the actual situation of human schizophrenia, the changes in myelin, neurotransmitters, and social behavior observed in our study can be strongly correlated with the pathophysiology of this disease. They may constitute an *in vivo* approach to study many aspects of such a complex human disorder and can also be used to screen drugs with potential treatment benefits.

Acknowledgment

Grant sponsor: The University of Buenos Aires; Grant number: UBA 20020100100395; Grant sponsor: The Agencia Nacional de Promoción de Ciencia y Tecnología PICT 0791, CONICET.

The authors are grateful to Dr. Modesto Rubio and Dr. Claudia García Bonelli for the dopamine determinations.

References

Aberg K, Saetre P, Jareborg N, Jazin E. 2006. Human QKI, a potential regulator of mRNA expression of human oligodendrocyte-related genes involved in schizophrenia. Proc Natl Acad Sci USA 103:7482–7487.

Achim AM, Ouellet R, Lavoie MA, Vallières C, Jackson PL, Roy MA. 2013. Impact of social anxiety on social cognition and functioning in patients with recent-onset schizophrenia spectrum disorders. Schizophr Res 145:75–81.

Adamo AM, Paez PM, Escobar Cabrera OE, Wolfson M, Franco PG, Pasquini JM, Soto EF. 2006. Remyelination after cuprizone-induced demyelination in the rat is stimulated by apotransferrin. Exp Neurol 198: 519–529.

Aleman A, Kahn RS, Selten JP. 2003. Sex differences in the risk of schizophrenia: Evidence from meta-analysis. Arch Gen Psychiatry 60:565–571.

Aston C, Jiang L, Sokolov BP. 2005. Transcriptional profiling reveals evidence for signaling and oligodendroglial abnormalities in the temporal cortex from patients with major depressive disorder. Mol Psychiatry 10:309–322.

Bénardais K, Kotsiari A, Skuljec J, Koutsoudaki PN, Gudi V, Singh V, Vulinović F, Skripuletz T, Stangel M. 2013. Cuprizone [bis(cyclohexylidenehydrazide)] is selectively toxic for mature oligodendrocytes. Neurotox Res 24:244–250.

Blank T, Prinz M. 2013. Microglia as modulators of cognition and neuropsychiatric disorders. Glia 61:62–70.

Braga RJ, Reynolds GP, Siris SG. 2013. Anxiety comorbidity in schizophrenia. Psychiatry Res 210:1–7.

Bradford MM. 1976. Rapid and sensitive method for the quantitation of microgram quantities of protein utilizing the principle of protein-dye binding. Anal Biochem 72:248–254.

Chen PS, Toribara T, Warner H. 1957. Microdetermination of phosphorus. Anal Chem 28:1756–1758.

Chew LJ, Fusar-Poli P, Schmitz T. 2013. Oligodendroglial alterations and the role of microglia in white matter injury: Relevance to schizophrenia. Dev Neurosci 35:102–129.

Dernovsek MZ, Sprah L. 2009. Comorbid anxiety in patients with psychosis. Psychiatr Danub 1:43–50.

Dracheva S, Davis KL, Chin B, Woo DA, Schmeidler J, Haroutunian V. 2006. Myelin-associated mRNA and protein expression deficits in the anterior cingulate cortex and hippocampus in elderly schizophrenia patients. Neurobiol Dis 21:531–540.

Duce JA, Podvin S, Hollander W, Kipling D, Rosene DL, Abraham CR. 2008. Gene profile analysis implicates Klotho as an important contributor to aging changes in brain white matter of the rhesus monkey. Glia 56:106–117.

Escobar Cabrera OE, Zakin MM, Soto EF, Pasquini JM. 1997. Single intracranial injection of apotransferrin in young rats increases the expression of specific myelin protein mRNA. J Neurosci Res. 47:603–608.

Franco PG, Silvestroff L, Soto EF, Pasquini JM. 2008. Thyroid hormones promote differentiation of oligodendrocyte progenitor cells and improve remyelination after cuprizone-induced demyelination. Exp Neurol 212:458–467.

Flynn SW, Lang DJ, Mackay AL, Goghari V, Vavasour IM, Whittall KP, Smith GN, Arango V, Mann JJ, Dwork AJ, Falkai P, Honer WG. 2003. Abnormalities of myelination in schizophrenia detected in vivo with MRI, and post-mortem with analysis of oligodendrocyte proteins. Mol Psychiatry 8:811–820.

Folch J, Lees M, Sloane Stanley GH. 1957. A simple method for the isolation and purification of total lipides from animal tissues. J Biol Chem 226:497–509.

Hakak Y, Walker JR, Li C, Wong WH, Davis KL, Buxbaum JD, Haroutunian V, Fienberg AA. 2001. Genome-wide expression analysis reveals dysregulation of myelination-related genes in chronic schizophrenia. Proc Natl Acad Sci USA 98:4746–4751.

Han M, Huang XF, Chen da C, Xiu MH, Hui L, Liu H, Kosten TR, Zhang XY. 2012. Gender differences in cognitive function of patients with chronic schizophrenia. Prog Neuropsychopharmacol Biol Psychiatry 39:358–363.

Heikkila RE, Hess A, Duvoisin RC. 1984. Dopaminergic neurotoxicity of 1-methyl-4-phenyl-1,2,5,6-tetrahydropyridine in mice. Science 224:1451–1453.

Hess HH, Lewin E. 1965. Microassay of biochemical structural components in nervous tissues: II Methods for cerebrosides proteolipid proteins and residue proteins. J Neurochem 12:205–211.

Hof PR, Haroutunian V, Friedrich VL Jr, Byne W, Buitron C, Perl DP, Davis KL. 2003. Loss and altered spatial distribution of oligodendrocytes in the superior frontal gyrus in schizophrenia. Biol Psychiatry 53:1075–1085.

Janssen J, Reig S, Parellada M, Moreno D, Graell M, Fraguas D, Zabala A, Garcia Vazquez V, Desco M, Arango C. 2008. Regional gray matter volume deficits in adolescents with first-episode psychosis. J Am Acad Child Adolesc Psychiatry 7:1311–1320.

Kaplan HI, Sadock BJ. 1971. Recent perspectives in schizophrenia. Can Psychiatr Assoc J 16:457–471.

Katsel P, Davis KL, Haroutunian V. 2005. Variations in myelin and oligodendrocyte-related gene expression across multiple brain regions in schizophrenia: A gene ontology study. Schizophr Res 79:157–173.

Laemmli UK. 1970. Cleavage of structural proteins during the assembly of the head of bacteriophage T4. Nature 227:680–685.

Lui S, Deng W, Huang X, Jiang L, Ouyang L, Borgwardt SJ, Ma X, Li D, Zou L, Tang H, Chen H, Li T, McGuire P, Gong Q. 2009. Neuroanatomical differences between familial and sporadic schizophrenia and their parents: An optimized voxel-based morphometry study. Psychiatry Res 171:71–81.

Makinodan M, Rosen KM, Ito S, Corfas G. 2012. A critical period for social experience-dependent oligodendrocyte maturation and myelination. Science 337:1357–1360.

Makinodan M, Yamauchi T, Tatsumi K, Okuda H, Takeda T, Kiuchi K, Sadamatsu M, Wanaka A, Kishimoto T. 2009. Demyelination in the juvenile period, but not in adulthood, leads to long-lasting cognitive impairment and deficient social interaction in mice. Prog Neuropsychopharmacol Biol Psychiatry 33:978–985.

Matsushima GK and Morell P. 2001. The neurotoxicant, cuprizone, as a model to study demyelination and remyelination in the central nervous system. Brain Pathol 11:107–116.

McGrath JA, Nestadt G, Liang KY, Lasseter VK, Wolyniec PS, Fallin MD, Thornquist MH, Luke JR, Pulver AE. 2004. Five latent factors underlying schizophrenia: Analysis and relationship to illnesses in relatives. Schizophr Bull 30: 855–873.

McGrath J, Saha S, Chant D, Welham J.2008. Schizophrenia: A concise overview of incidence, prevalence, and mortality. Epidemiol Rev 30:67–76.

Meyer U, Murray PJ, Urwyler A, Yee BK, Schedlowski M, Feldon J. 2008. Adult behavioral and pharmacological dysfunctions following disruption of the fetal brain balance between pro-inflammatory and IL-10-mediated anti-inflammatory signaling. Mol Psychiatry 13:208–221.

Murray RM, Jones P, O'Callaghan E, Takei N, Sham P. 1992. Genes, viruses and neurodevelopmental schizophrenia. J Psychiatr Res 26:225–235.

Norton WT, Poduslo SE. 1973. Myelination in rat brain:method of myelin isolation. J Neurochem 21:749–757.

Novak G, Fan T, O'Dowd BF, George SR. 2013. Striatal development involves a switch in gene expression networks, followed by a myelination event: Implications for neuropsychiatric disease. Synapse. 67:179–188.

Patel AB, Hays SA, Bureau I, Huber KM, Gibson JR. 2013. A target cell-specific role for presynaptic Fmr1 in regulating glutamate release onto neocortical fast-spiking inhibitory neurons. J Neurosci 33:2593–2604.

Paxinos G, Watson C. 1986. The Rat Brain in Stereotaxic Coordinates. Academic Press.

Rajkowska G, Miguel-Hidalgo JJ, Wei J, Dilley G, Pittman SD, Meltzer HY, Overholser JC, Roth BL, Stockmeier CA. 1999. Morphometric evidence for neuronal and glial prefrontal cell pathology in major depression. Biol Psychiatry 45:1085–1098.

Rosato Siri MV, Badaracco ME, Pasquini JM. 2013. Glatiramer promotes oligodendroglial cell maturation in a cuprizone-induced demyelination model. Neurochem Int 63:10–24.

Rosin C, Colombo S, Calver AA, Bates TE, Skaper SD. 2005. Dopamine D2 and D3 receptor agonists limit oligodendrocyte injury caused by glutamate oxidative stress and oxygen/glucose deprivation. Glia 52:336–343.

Schneider T, Przewłocki R. 2005. Behavioral alterations in rats prenatally exposed to valproic acid: Animal model of autism. Neuropsychopharmacology 30:80–89.

Schneiderman JS, Buchsbaum MS, Haznedar MM, Hazlett EA, Brickman AM, Shihabuddin L, Brand JG, Torosjan Y, Newmark RE, Canfield EL, Tang C, Aronowitz J, Paul-Odouard R, Hof PR. 2009. Age and diffusion tensor anisotropy in adolescent and adult patients with schizophrenia. Neuroimage 45: 662–671.

Shimizu S, Koyama Y, Hattori T, Tachibana T, Yoshimi T, Emoto H, Matsumoto Y, Miyata S, Katayama T, Ito A, Tohyama M. 2014. DBZ, a CNS-specific DISC1 binding protein, positively regulates oligodendrocyte differentiation. Glia 62:709–724.

Simon P, Dupuis R, Costentin J. 1994. Thigmotaxis as an index of anxiety in mice. Influence of dopaminergic transmissions. Behav Brain Res 61:59–64.

Smith RS. 1992. A comprehensive macrophage-T-lymphocyte theory of schizophrenia. Med Hypotheses 39:248–257.

Stewart DG, Davis KL. 2004. Possible contributions of myelin and oligodendrocyte dysfunction to schizophrenia. Int Rev Neurobiol 59:381–424.

Stidworthy MF, Genoud S, Suter U, Mantel N, Franklin RJM. 2003. Quantifying the early stages of remyelination following cuprizone-induced demyelination. Brain Pathol 13:329–339.

Takahashi N, Sakurai T, Davis KL, Buxbaum JD. 2011. Linking oligodendrocyte and myelin dysfunction to neurocircuitry abnormalities in schizophrenia. Prog Neurobiol 93:13–24.

Tkachev D, Mimmack ML, Ryan MM, Wayland M, Freeman T, Jones PB, Starkey M, Webster MJ, Yolken RH, Bahn S. 2003. Oligodendrocyte dysfunction in schizophrenia and bipolar disorder. Lancet 362:798–805.

Torrey EF, Webster M, Knable M, Johnston N, Yolken RH. 2004. The Stanley foundation brain collection and neuropathology consortium. Schizophr Res 44:151–155.

Uranova NA, Vikhreva OV, Rachmanova VI, Orlovskaya DD. 2011. Ultrastructural alterations of myelinated fibers and oligodendrocytes in the prefrontal cortex in schizophrenia: A postmortem morphometric study. Schizophr Res Treat 2011:13, Article ID 325789.

Uranova NA, Vostrikov VM, Orlovskaya DD, Rachmanova VI. 2004. Oligodendroglial density in the prefrontal cortex in schizophrenia and mood disorders: A study from the Stanley Neuropathology Consortium. Schizophr Res 67: 269–275.

Weinberger DR. 1995. From neuropathology to neurodevelopment. Lancet 346:552–557.

Wright P, Murray RM. 1993. Schizophrenia: Prenatal influenza and autoimmunity. Ann Med 25:497–502.

Yu H, Bi W, Liu C, Zhao Y, Zhang D, Yue W. 2014. A hypothesis-driven pathway analysis reveals myelin-related pathways that contribute to the risk of schizophrenia and bipolar disorder. Prog Neuropsychopharmacol Biol Psychiatry 51C:140–145.

Zhu H, Zhao L, Wang E, Dimova N, Liu G, Feng Y, Cambi F. 2012. The QKI-PLP pathway controls SIRT2 abundance in CNS myelin. Glia 60:69–82.